Reinterpretation of resistivity and induced polarization data to explore gold mineralization zones at Zarzima prospect, Iran

Seyyed Reza Mashhadi[1], Meysam Nikfarjam[1] & Ahmad Kazemi Mehrnia[2]

[1] Department of Mining and Metallurgical Engineering, Amirkabir University of Technology (Tehran Polytechnic), 424 Hafez Ave, 15875-4413 Tehran, Islamic Republic of Iran; reza.mashhadi93@aut.ac.ir , reza.mashhadi93@yahoo.com
[2] Parsi Kan Kav Engineering Consultant Company, Eastern Arash Blvd, Farid Afshar St., Shariati Ave., 191986-5956 Tehran, Islamic Republic of Iran

AGEOS

Abstract: Zarzima is a gold prospect located in the west of Muchesh city, Kurdistan province, Iran. According to the geological studies, gold mineralization mainly occurs within silicified alteration zones/quartz veins and veinlets. Some silicified veins have been mapped in the 1:1,000 geological map of the area. To improve the results of drillings, resistivity and induced polarization tomography surveys were performed before the exploration drillings in the study area. As the geophysical models didn't really coincide with the geological information, we have decided to reprocess and reinterpret the previously recorded geophysical data with further theoretical considerations. Interesting results yielded with suitable inversion criteria and precise data processing. This investigation indicated that high resistivity anomalies represent silicified alteration zones. In fact, some branch-like high resistivity features are detected which is consistent with the hydrothermal mineralization systems. The fault zone is also characterized precisely in the resistivity and IP models. Note that previous analysis of geophysical data neglected the most important anomalous zone in the study area. The previous analysis also didn't reveal the branch-like structures and the fault zone. These facts clearly show the importance of suitable selection of inversion parameters and also avoiding the use of large "n" values in the dipole-dipole array. In the end, it should be noted that a suitable combination of larger "a" values and smaller "n" values (non-integer) for the dipole-dipole array can guarantee deeper depth of investigation and higher signal quality concurrently in an electrical survey.

Key words: gold exploration, resistivity, induced polarization (IP), silicified alteration, Zarzima, Iran

1. INTRODUCTION

The exploration of gold deposits is usually performed by means of geological and geochemical methods. These methods are often limited to surface characterizations and cannot provide reliable information about the subsurface variations, especially for the majority of gold deposit types that follow complicated patterns in the deposit scale since the gold itself is nearly always irregularly distributed in the deposit (Pohl, 2011). In some of the deposit types (i.e. hydrothermal vein-type, orogenic, etc.), the mineralization zone cannot be tracked effectively even after drilling the exploration boreholes. This complexity may lead to a situation that the main mineralization zones remain hidden (an example can be found at Wang et al., 2013). Interestingly, the use of suitable geophysical methods can extremely assist the explorers to have a better understanding about the area by scanning the subsurface for finding spatial patterns, structural features, promising zones and so on that can be used for tracking the mineralization both in horizontal and vertical directions. Furthermore, geophysical methods can be successfully used when geological and geochemical methods are limited, such as the case that the mineralization zones or the favourable lithological units are concealed (Robert et al., 2007; Reynolds, 2011; Hope & Anderson, 2016).

Harkönen & Keinänen (1989) reported the use of airborne magnetic, electromagnetic, and radiometric measurements for regional exploration of structurally controlled gold deposits. They reported that the most amenable techniques for locating the gold mineralization zones have been the lithogeochemistry and IP methods. Freebrey et al. (1998) have found the capability of regional gravity data together with high-resolution aeromagnetic and radiometric measurements to detect low sulphidation epithermal Au-Ag deposits in Japan. In the detailed exploration stage, Park et al. (2009) showed that gold mineralization hosted by quartz veins are detectable by low resistivity responses since almost all of the gold mineralization occurs in fractured areas associated with faults or shear zones. On the contrary, Invine & Smith (1990) expressed that gold-bearing silicified zones and shallow quartz veins in the epithermal gold mineralization systems are commonly detectable by resistivity technique as they are highly resistive. Robert et al. (2007) presented interesting notes about gold mineralization models and the use of different methods in gold exploration. They pinpointed the importance of 3D geophysical modeling i.e. 3D inversion of potential field data. Furthermore, they expressed that resistivity method is commonly used in sedimentary environments where high resistivity intrusions and silicified alteration zones can be mapped in less resistive carbonaceous and non-carbonaceous sedimentary units.

In this paper, it is tried to use electrical resistivity and induced polarization methods for gold exploration in Zarzima

Manuscript received 2019-07-29
Revised version accepted 2020-04-07

prospect, west of Iran. Although the real deposit type is still unrecognized due to great complexities, it is estimated to be an orogenic gold deposit (further investigations are still going on in the area). Basically, we hoped to identify silicified zones promising for gold mineralization and also possible metallic sulfide occurrences within the prospect in order to prioritize exploration drillings going on in the area. In fact, we have re-processed and reinterpreted a previously recorded geophysical data with further theoretical considerations (previous analysis was not really consistent with available geological data). If these considerations are followed, a reliable electrical model will be resulted that can assist us to have a realistic understanding of the geological structures; otherwise, an unreliable model will be resulted. This investigation showed that the presented models are more consistent with the available geological data, and, the previous study would lead to unrealistic results. In the following sections, after a relatively brief site description, the electrical data analysis is discussed in detail.

2. GEOLOGICAL SETTING OF ZARZIMA PROSPECT

The Zarzima gold prospect is located 30 km southeast of Sanandaj city, Kurdistan province, western Iran. It is located in a rugged topographic terrain in the west of Muchesh city (Fig. 1).

The study area is located in the Zagros orogenic belt. This belt consists of three subzones: Urumieh Dokhtar Magmatic Arc (UDMA), Sanandaj-Sirjan Zone (SSZ), and Zagros Folded Belt (ZFB) (Alavi, 1994). SSZ is a NW–SE trending zone that extends from northwest to southwest of Iran and has more than 200 Km width and about 1500 km length (Stocklin, 1968). The SSZ is a zone of thrust faults that have transported slices of

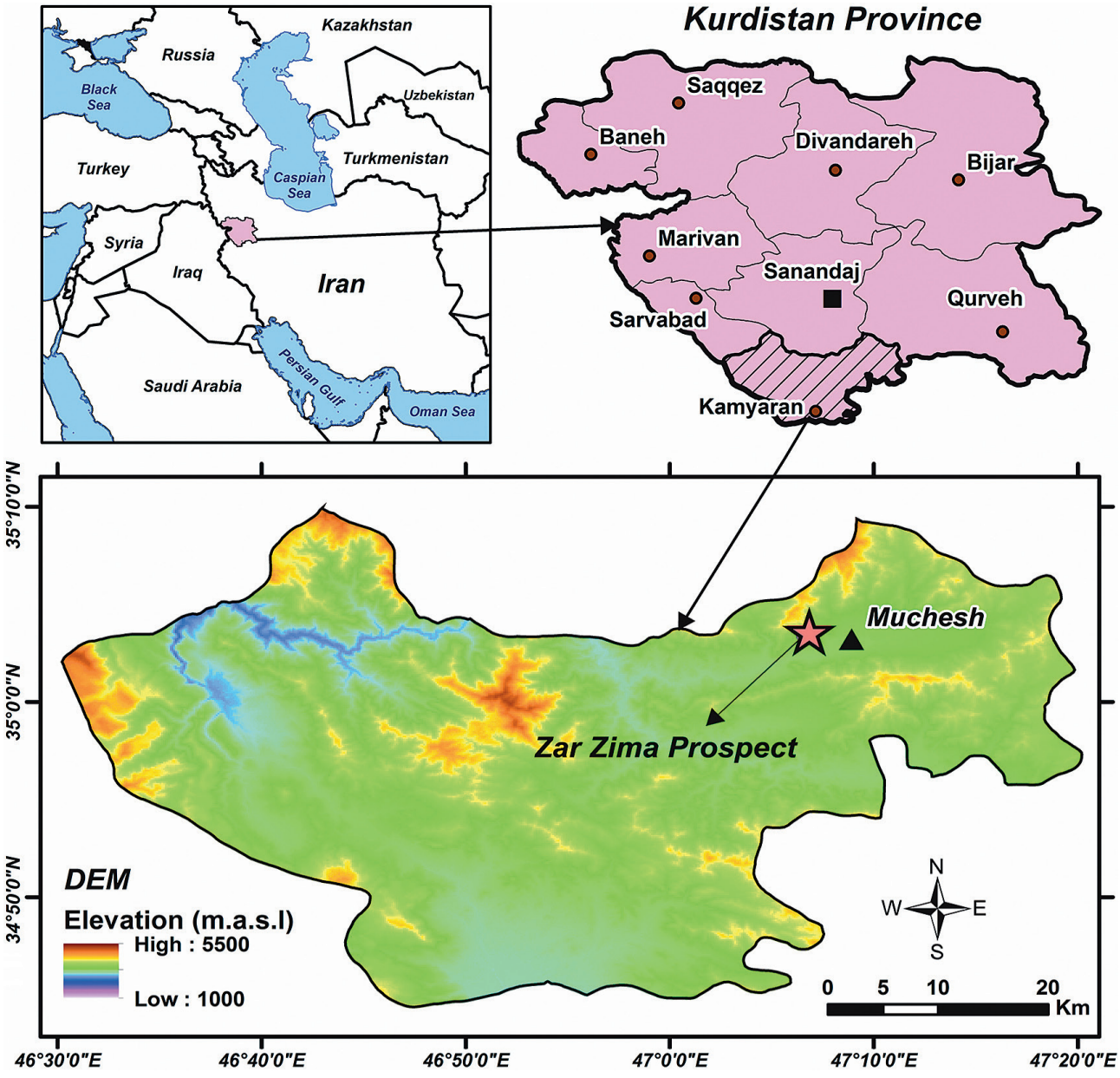

Fig. 1. Location of Zarzima prospect in the west of Muchesh city, Kurdistan Province, Iran.

metamorphosed and non-metamorphosed Phanerozoic stratigraphic units of the Afro-Arabian passive continental margin. The zone consists of metamorphic and greatly deformed rocks associated with abundant deformed and undeformed plutons in addition to widespread Mesozoic volcanic rocks (Aliyari et al., 2012). The SSZ hosts at least five main gold deposits including orogenic gold (i.e. Qolqoleh, Kervian, Qabaqloujeh, Kharapeh, and Alut), epithermal gold (i.e. Aghdarreh, Sari Gunay, and Gozalbolagh), Carlin-type (i.e. Zarshuran, Akhtarchi), intrusion-related (i.e. Muteh, Astaneh, and Zartorosht), and gold-rich volcanic-hosted massive sulphide (VMS) (i.e. Barika) (Aliyari et al., 2012).

In Zarzima prospect, geological features are mapped at a 1:1000 scale (Fig. 2). Base on stratigraphy, the oldest rock unit in the study area is formed during the Early Cretaceous. This geological unit consists of thick limestone and marl that are folded in most cases. The volcano-sedimentary units are widespread in the study area. The geological mapping indicated that volcano-sedimentary rocks host silicified veins. Silicified zones/quartz vein and veinlets are the most common features that host gold mineralization. Other minerals include metallic sulphides (mainly pyrite, galena, chalcopyrite, etc.), iron oxides (mainly hematite), malachite, calcite, and barite. From the tectonic point of view, two main trends of faults are NW–SE and NE–SW. Despite the performed exploration activities, the real deposit type is not exactly recognized since the geological setting is complicated and the geochemical behavior of gold within the area is not entirely understood. Further investigations are going on to understand the gold mineralization characteristics in detail.

3. GEOPHYSICAL INVESTIGATION: 2D RESISTIVITY AND INDUCED POLARIZATION TOMOGRAPHY

3.1. Data Acquisition

In order to delineate subsurface features especially the gold-bearing quartz veins/silicified alteration zones, electrical resistivity and Induced Polarization (IP) tomography through the two-dimensional survey was performed. Five profiles were completed to study the area (Fig. 2). As the veins and alteration zones are likely to be steep in our study area, the dipole-dipole array is used which is well suited for mapping vertical structures (Loke, 2018). The dipole-dipole array is a well-known beta-type electrodes configuration (C1-C2-P1-P2). In this array, spacing between current electrodes (C1-C2), which is referred to as the parameter "a", is the same as the spacing between potential electrodes (P1-P2). The spacing between the second current electrode and the first potential electrode (C2-P1) is "n" times as much as "a".

The GDD IP-transmitter (model: TX III) and GRX2 receiver were used for data measurements. Induced Polarization (IP) measurements are done by a current pulse of 2 seconds

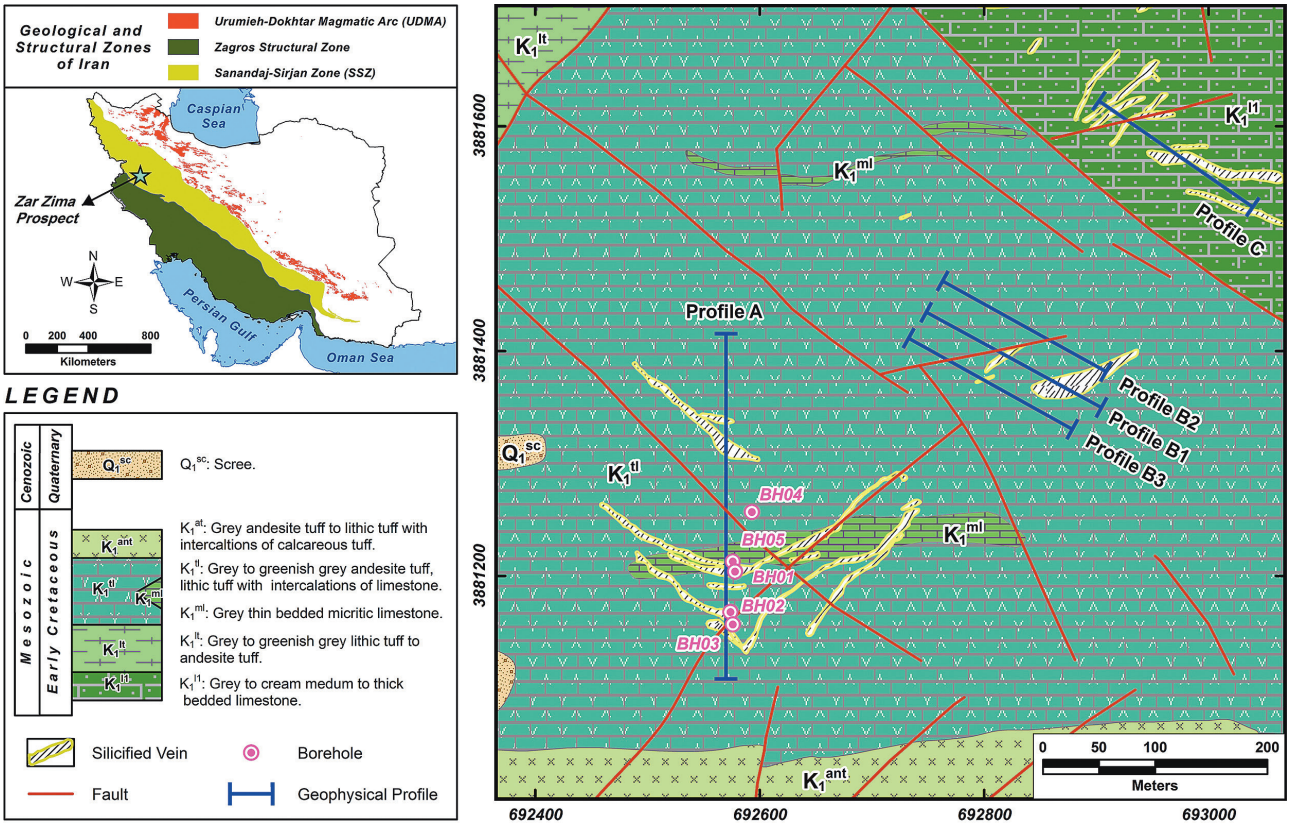

Fig. 2. The 1:1,000 geological map of Zarzima area together with the resistivity and Induced Polarization (IP) profiles. The location of the study area in the Sanandaj-Sirjan Zone is also shown.

(2 seconds on and 2 seconds off). In the geophysical dataset of the Zarzima area, the measurements of one IP-window is only available (delay time: 240 ms, integration time: 80 ms). The recorded dataset involves dipole-dipole readings with "n" parameter ranging from 1 to 11 with the potential dipole spacing of 10 m. Note that only n = 1 to n = 6 is used in this investigation for the inverse modeling process since many researchers in the literature have avoided the use of large "n" values in the dipole-dipole array i.e. Loke (2018) and Rucker et al. (2011). Furthermore, we have provided some insights based on repeated reading errors to further prove this fact.

3.2. Analysis of Repeated Readings

Geophysicists should always consider the sources of noise while designing a survey or processing the geophysical datasets in order to have an eye for the possible artifacts and/or inaccuracies in the models. In electrical resistivity surveys, it is common to remove noisy data prior to inverse modeling process to prevent modeling artifacts (i.e. Mashhadi et al., 2019). Absolute and relative errors are the two factors for assessing the signal to noise ratio (S/N) in an electrical survey. Absolute error is defined as "the absolute difference of two repeated readings" while relative error is "the absolute difference of two repeated readings divided by their mean value" (Loke, 2018; Rucker et al., 2011).

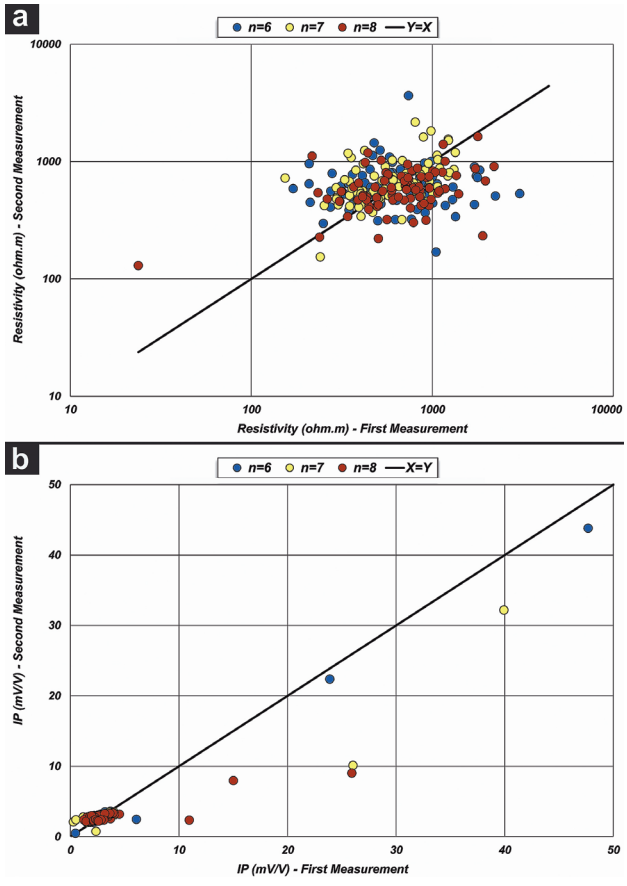

Fig. 3. Scatter plots showing the repeated measurements of apparent resistivity (a) and apparent IP (b) for n = 6 – 8 values. Note that the total number of 251 readings are repeated.

According to the available dataset, repeated readings are only available for n = 6 to n = 8 due to the used data acquisition scenario. Basically, the dipole-dipole readings for n = 1 – 8 were recorded in the first stage and then the readings were performed for n = 6 – 11. This gives us the opportunity to access the errors for some of "n" values. Total number of repeated readings was 251. These repeated measurements of resistivity and IP are plotted in scatter plots to provide a better illustration of the data (Fig. 3). Fig. 3 indicates that resistivity measurements are pretty noisy for all of the n values. However, IP measurements seem to be good with only a few extremely noisy measurements. This is not expected as IP measurements are far more susceptible to noise than the resistivity data (Dahlin et al., 2002; Loke, 2018; Mashhadi & Ramazi, 2018). This phenomenon can be explained by the low values of IP readings where only 8 out of 251 IP readings are higher than 10mV/V. Note the better quality of IP data for n = 6 with respect to n = 7 and n = 8.

Absolute and relative errors are also calculated for both resistivity and IP parameters. Finally, to have a better comparison, the mean values are plotted in a diagram (Fig. 4). For resistivity, the mean values of absolute errors are high for all of "n" values. Unexpectedly, the maximum occurs for n = 6. However, this problem could be explained by relative errors being the smallest for n = 6. In fact, there are a few extremely noisy measurements in which the absolute error exceed 1000 ohm.m. These noisy measurements lead to a dramatic increase in the mean value. On the whole, the data recorded for all of "n" values are contaminated with some level of noise, being higher for n = 7 and n = 8 (on average, 15% higher than n = 6). For chargeability/IP measurements, both of the absolute and relative errors indicate a significant increase from n = 6 to n = 8. Note that low absolute errors are due to little IP variations in the subsurface where it is almost constant in four profiles (just profile A has a considerable IP variation). Also, note that the absolute error for IP was high for a few data points. The maximum value of the IP absolute error equals with 16.9 mV/V for a measurement with n = 7, which disrupted the general trend from n = 6 to n = 8. Although these facts can further prove the unreliability of high "n" values for the dipole-dipole array (n = 7

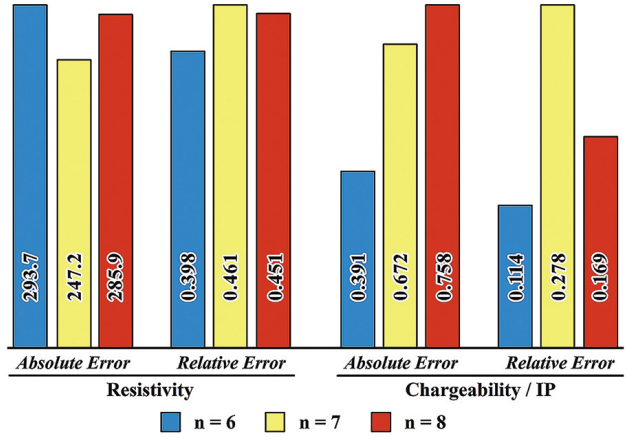

Fig. 4. A diagram showing the mean values of the absolute and relative errors for resistivity and chargeability (IP) measurements based on repeated readings that are calculated for n = 6 – 8. Note that the measurements from all of the geophysical profiles are included in the calculations.

and n = 8 based on this comparison), it seems that these numbers cannot clearly represent the real differences in measurement stability and/or noise contamination since:

1. theoretically, the voltage is inversely proportional to the cube of the "n" factor in the dipole-dipole array (Loke, 2018). Accordingly, the signal strength/voltage is 37% lower for n = 7 with respect to n = 6, and, this value is 58% for n = 8. Consequently, the low differences between the calculated errors for different "n" values do not reveal the whole story.
2. this method of comparison about the noise contamination for high and low "n" values in the dipole-dipole array is better to be performed when we are sure about good electrodes contact. Extremely noisy measurements can be the result of bad contact between the electrodes and the multicore cable (Dahlin et al., 2002) or between the electrodes and the ground. Poor electrode contact is not easily recognized in the field, and, sometimes it affects a series of measurements instead of one single recording. Thus, it strongly affects the mean value of the calculated errors.
3. other parameters can also play an important role in the calculated errors including the measurement instrument, type of electrodes used (Dahlin et al., 2002; LaBrecque & Daily, 2008), the measurement sequence used in automatic data measurement systems (Dahlin, 2000), etc.

On the whole, this simple error calculation showed the great differences in noise levels for "n" values ranging from 6 to 8. The noise contamination for IP data clearly shows a remarkable increase from n = 6 to n = 8. This fact implies that using high "n" values in the dipole-dipole array just provides a highly contaminated/noisy data, even if a modern instrumentation is utilized for data acquisition. This fact can also be proposed for similar arrays like pole-dipole and pole-pole. As a result, it is better to use large "a" spacing rather than high "n" values while trying to increase the depth of investigation. The required resolution in this scenario can be achieved by recording more measurements such as using non-integer "n" values and/or combining the measurements of several "a" spacings into a single dataset.

3.3. Data Inversion & Model Interpretations

The measured data is inverted by using the Res2dinv software (commercially available at geotomosoft.com). The "smoothness-constrained least-squares optimization" method is used for data inversion as it is expected to have a gradual resistivity variation. Dipole-dipole readings with n = 1 to n = 6 are used. According to the considerations mainly noted by Loke (2018) and Hauck & Kneisel (2008), the following criteria are selected for data inversion: initial damping factor = 0.17, minimum damping factor = 0.02, damping factor optimization enabled by using the "L-curve method", 4 nodes used between adjacent electrodes, software default parameters for the stopping criteria, unit electrode spacing = 5 m, cell size in the z-direction increases with the factor of 1.05 and the first block is 2.5 m, and the topography is incorporated into the inversion process by the "distorted finite-element grid with damped distortion" option.

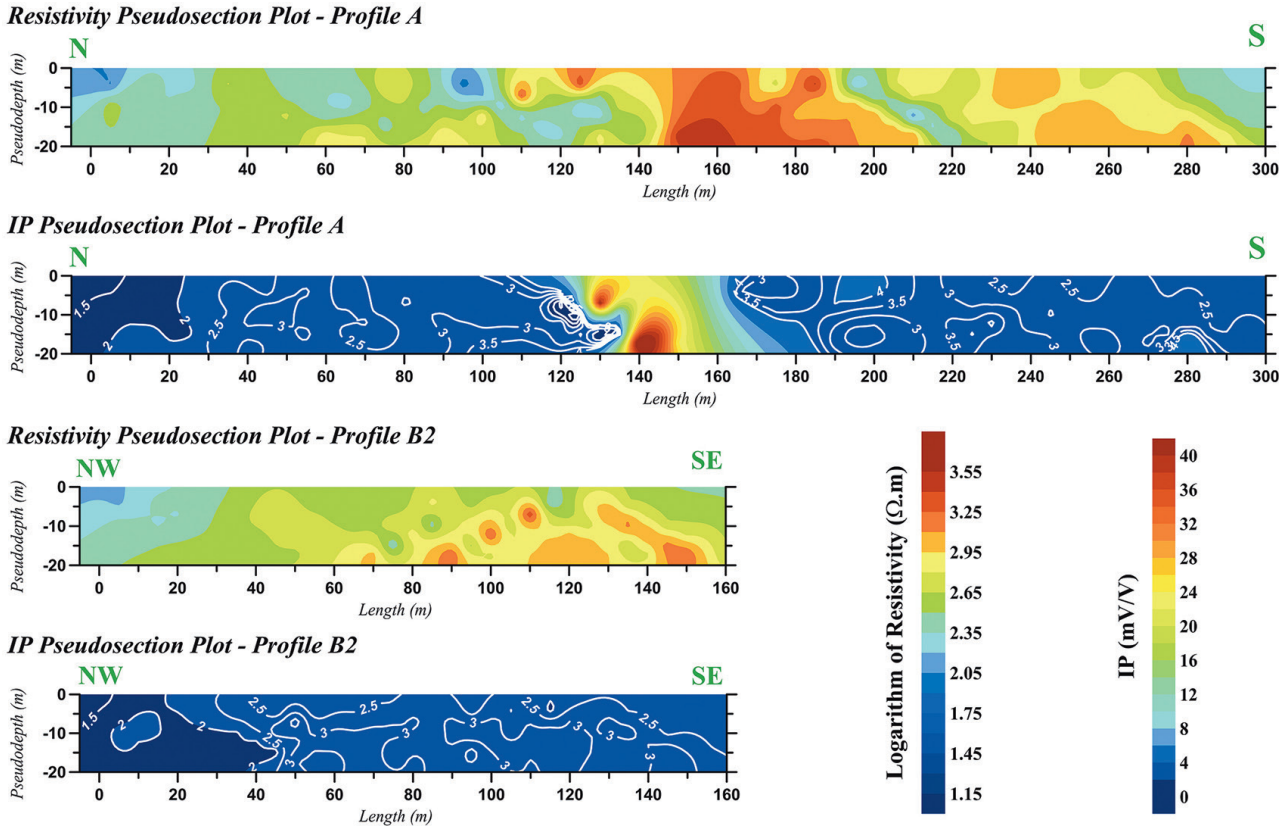

Fig. 5. Pseudosection plots of resistivity and IP for Profile A and Profile B2.

The inversion models seem to be reliable and realistic as the geological data is consistent with the presented models. As all of the models followed basic interpretational facts and also pretty similar structures, only the results of profile A and B2 are presented in this paper. The inversion of profile A and B2 is completed after 5 iterations. As the features are repeated in subsequent iterations, the model credibility is proven somehow (Hauck & Kneisel, 2008). The pseudosection plots of these profiles are also shown at Fig. 5. For profile A, the resistivity and IP models of the iteration 4 are selected for final interpretations with the rms errors of 18.8 and 3.1 for the resistivity and IP models, respectively. The results of iteration 5 is considered for profile B2 with the rms errors of 19.2 and 0.2 for the resistivity and IP models. Note the low rms error of IP model in profile B2 is related to the very low variations of IP measurements.

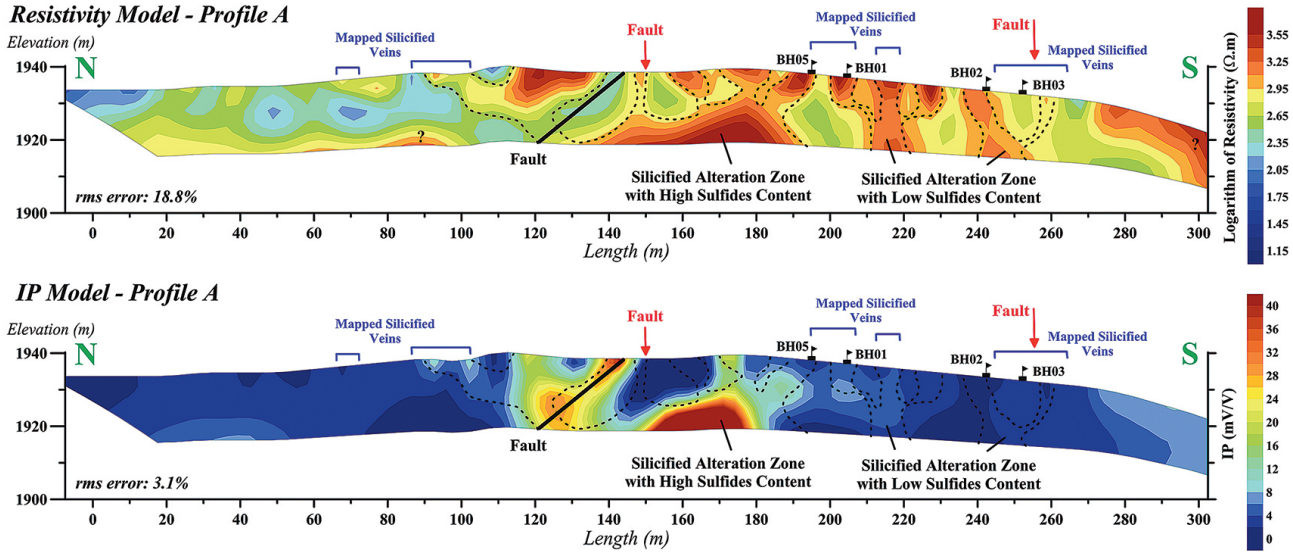

Fig. 6. Inverted resistivity and IP models of Profile A. The dashed lines represent an approximate boundary for the silicified alteration zone (promising zones for gold mineralization).

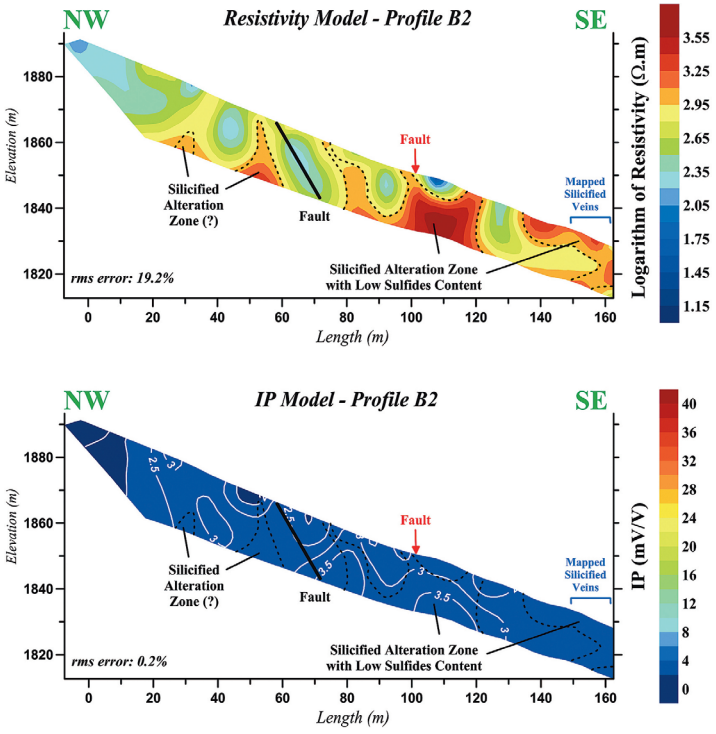

Fig. 7. Inverted resistivity and IP models of Profile B2. The dashed lines represent an approximate boundary for the silicified alteration zone (promising zones for gold mineralization). Note that some IP contours are selected and shown with white lines for a better representation of low IP variations.

The inverted resistivity and IP models of profile A and profile B2 are shown together with interpretational notes in Figs. 6 and 7, respectively. Note that the descriptions written on the surface of the sections are taken from the 1:1,000 geological map of Zarzima prospect to evaluate the geophysical models. The notes written below the sections are related to geophysical interpretation results.

There are four boreholes on this profile but a correlation between resistivity and IP models with the boreholes is really difficult if not impossible. That's because: (1) lithology characterization was really challenging as the geologists mentioned, and, in some cases the lithology was detected with high uncertainties, and more importantly (2) quartz veins and veinlets are small in dimensions, irregularly occurring within different rocks and no clear silicified alteration zone could be delineated i.e. no proper classification could be made. On the other hand, these boreholes have provided a fact which could support the IP model of profile A since a considerable amount of metallic sulfides (mainly pyrite, galena and chalcopyrite) observed in BH01 and BH05 whereas the observed metallic sulfides in BH02 and BH03 was almost negligible. Being closer to the main IP anomaly together with an increase in IP response below BH01 and BH05 can explain the higher amount of sulfide minerals at this location. Note that previous

geophysical analysis was not really consistent with the geological data and drilled boreholes.

As the geophysical models show, high resistivity values represent silicified alteration zones. The outcrops of silicified veins are somehow consistent with high resistivity features, indicating the validity of the resistivity model. Note that some boundaries are drawn for the silicified alteration zones but these boundaries just represent "approximate limits" since the resolution of the dataset is not that high to be able to map these alteration zones accurately with high precision. In fact, the boundaries are drawn to show that the anomaly shapes are consistent with a hydrothermal mineralization event (the branch-like structure). It must be noted that there is no evidence of "smearing out with depth" for these high resistivity anomalies, which can further assure us of the represented branch-like features. In addition to anomaly shapes, existing boreholes can approve the interpretations since irregularly distributed quartz veins and veinlets were reported in all of the boreholes especially in BH01 and BH05.

There is a low resistivity zone at about 140 m which coincides with a high IP anomaly. This seems to be related to a fault zone which is also mapped in the geological survey. The fault zone is less resistive and also more chargeable than the surrounding rocks due to high clay content and/or high moisture content. The same geophysical responses in the fault zones are reported by Mashhadi et al. (2017). However, the location of this fault seems to be a bit inaccurate in the geological map and should be corrected. The other mapped fault at about 255 m did not appear in the geophysical models. The reason is not clearly understood and no contributions can be proposed with high certainty. This fault is better to be checked again by the geologists. Adjacent to the detected fault, at about 170 m, there is a high IP anomaly consistent with a high resistivity feature. It is contributed that this location is a highly silicified alteration zone with a considerable amount of metallic sulfides. It is not really known that gold mineralization coexists with metallic sulfides or not. However, as the resistivity values are really high, it is expected to have strong silicified alteration zone with lots of quartz veins and veinlets, which in turn, is expected to have gold mineralization. Hence, this anomaly is better to be checked by exploration drilling as it seems to be the most important promising zone in the area (based on the geophysical investigation).

In profile B2, similar structures and interpretations can be proposed. High resistivity anomalies seems to be the response of silicified alteration zones. The mapped fault seems to be inaccurate. It is probably related to geological mapping difficulties in the area i.e. soil cover, complicated geological structures, etc. Another important point is that IP values are almost constant with very low variations. This fact indicates that sulfide minerals are almost absent or they occur in very low contents within the rock units beneath profile B2.

Previous analysis of geophysical data neglected the most important anomalous zone at Zarzima prospect. The previous analysis also didn't reveal the branch-like structures and the fault zone. These facts clearly show the importance of suitable selection of inversion parameters and also avoiding the use of large "n" values in the dipole-dipole array.

4. CONCLUSIONS

In this paper, the previously recorded geophysical data (including resistivity and IP) at Zarzima prospect is reprocessed and reinterpreted since previously performed analysis didn't coincide with the available geological information. Interesting results yielded with suitable inversion criteria. Although the raw dataset involves the dipole-dipole readings with "n" ranging from 1 to 11, only up to n = 6 is used in this paper. Furthermore, according to the available repeated readings, absolute and relative errors for resistivity and chargeability/IP are calculated for n = 6 to n = 8. Finally, it is shown that high "n" values in the dipole-dipole measurements are susceptible to higher noise levels and therefore must be avoided in the geophysical analysis. The provided models after suitable inversion criteria lead to reliable resistivity and IP models that are consistent with the geological information. This investigation indicated high resistivity features represent silicified alteration zones. In fact, some branch-like high resistivity features are detected which is consistent with the hydrothermal mineralization systems. The fault zone is also characterized precisely in the resistivity and IP models. The subsurface structures seem to be mapped accurately so it clearly shows the importance of suitable selection of inversion parameters and also avoiding the use of large "n" values in the dipole-dipole array. So care must be taken seriously in project design, data processing and final interpretations to provide a realistic result.

Acknowledgment: We thank our colleagues from Parsi Kan Kav Engineering Consultant Company who provided insight and expertise that greatly assisted the research. We also appreciate the geophysical team for their efforts in the field data acquisition.

References

Alavi M., 1994: Tectonics of the Zagros orogenic belt of Iran: new data and interpretations. Tectonophysics, 229, 211–238.

Aliyari F., Rastad E. & Mohajjel M., 2012: Gold Deposits in the Sanandaj–Sirjan Zone: Orogenic Gold Deposits or Intrusion-Related Gold Systems. Resource Geology, 62, 296–315.

Dahlin T., 2000: Short note on electrode charge-up effects in DC resistivity data acquisition using multi-electrode arrays. Geophysical Prospecting, 48, 181–187.

Dahlin T., Leroux V. & Nissen J., 2002: Measuring techniques in induced polarisation imaging. Journal of Applied Geophysics, 50, 279–298.

Freebrey C.A., Hishida H., Yoshika K. & Nakayama K., 1998: Geophysical Expression of Low Sulphidation Epithermal Au-Ag Deposits and Exploration Implications – Examples from the Hokusatsu Region of SW Kyushu, Japan. Resource Geology, 48, 2, 75–86.

Harkönen I. & Keinänen V., 1989: Exploration of structurally controlled gold deposits in the central Lapland Greenstone Belt. Geological Survey of Finland, Special Paper, 10, 79–82.

Hauck C. & Kneisel C., 2008: Applied geophysics in periglacial environments. Cambridge University Press.

Hope M. & Andersson S., 2016: The discovery and geophysical response of the Atlántida Cu–Au porphyry deposit, Chile. Exploration Geophysics, 47, 3, 237–247.

Irvine R.J. & Smith M.J., 1990: Geophysical exploration for epithermal gold deposits. Journal of Geochemical Exploration, 36, 375–412.

LaBrecque D. & Daily W., 2008: Assessment of measurement errors for galvanic-resistivity electrodes of different composition. Geophysics, 73, 2, F55–F64.

Loke M.H., 2018: Tutorial: 2-D and 3-D electrical imaging surveys. (Revision date: 6th March 2018), (www.geotomosoft.com).

Mashhadi S.R. & Ramazi H., 2018: The Application of Resistivity and Induced Polarization Methods in Identification of Skarn Alteration Haloes: a Case Study in Qale-Alimoradkhan Area: Journal of Environmental & Engineering Geophysics, 23, 3, 363–368.

Mashhadi S.R., Mostafaei K. & Ramazi H., 2017: Improving bitumen detection in resistivity surveys by using induced polarization data: Exploration Geophysics, 49, 5, 762–774.

Mashhadi S.R., Ramazi H. & Asgarpour Shahreza M., 2019: Assessing the effects of 1D assumption violation in vertical electrical sounding (VES) data processing and interpretation: Acta Geophysica, 68, 105–122.

Park J., You Y. & Kim H., 2009: Electrical resistivity surveys for gold-bearing veins in the Yongjang mine, Korea. Journal of Geophysics and Engineering, 6, 73–81.

Pohl W.L., 2011: Economic geology, Principles and Practice. Wiley-Blackwell, Chichester, UK, 663 p.

Reynolds J.M., 2011: An Introduction to Applied and Environmental Geophysics. 2nd edition, John Wiley & Sons, UK, 710 p.

Robert F., Brommecker R., Bourne B.T., Dobak P.J., McEwan C.J., Rowe R.R. & Zhou X., 2007: Models and exploration methods for major gold deposit types. In: Milkereit B. (Ed.), Proceedings of Exploration 07: Fifth Decennial International Conference on Mineral Exploration, pp. 691–711.

Rucker D.F., Noonan G.E. & Greenwood W.J., 2011: Electrical resistivity in support of geological mapping along the Panama Canal. Engineering Geology, 111, 121–133.

Stocklin J., 1968: Structural History and Tectonics of Iran: A Review. AAPG Bulletin, 52, 1229–1258.

Wang C., Carranza E.J., Zhang S., Zhang J., Liu X., Zhang D., Sun X. & Duan C., 2013: Characterization of primary geochemical haloes for gold exploration at the Huanxiangwa gold deposit, China. Journal of Geochemical Exploration, 124, 40–58.